




Debris flow susceptibility and propagation assessment in West Koyulhisar, Turkey

Ali POLAT ^{1*}  <https://orcid.org/0000-0002-9147-3633>;  e-mail: ali.polat@afad.gov.tr

Dursun ERİK²  <https://orcid.org/0000-0001-8884-5443>; e-mail: dursunerik@gmail.com

*Corresponding author

¹ Provincial Directorate of Disaster and Emergency, Sivas 58050, Turkey

² Republic of Turkey General Directorate of Highway, 16. District, Sivas 58049, Turkey

Citation: Polat A, Erik D (2020) Debris flow susceptibility and propagation assessment in West Koyulhisar, Turkey. Journal of Mountain Science 17(11). <https://doi.org/10.1007/s11629-020-6261-6>

© Science Press, Institute of Mountain Hazards and Environment, CAS and Springer-Verlag GmbH Germany, part of Springer Nature 2020

Abstract: Turkey is highly prone to landslides because of the geological and geographic location. The study area, which is located in a tectonically active region, has been significantly affected by mass movements. Flow type landslides are frequently observed due to this location. This study aims at determining the source area and propagation of debris flows in the study area. We used the heuristic method to extract source areas of debris flow, and then used receiver operating characteristic (ROC) curve analysis to assess the performance of the method, and finally calculated the Area under curve (AUC) values being 83.64% and 80.39% for the success rate and prediction rate, respectively. We calculated potential propagation area and runout distance with Flow-R software. In conclusion, the obtained results (susceptibility map, propagation and runout distance) are very important for decision-makers at the region located on an active fault zone, which is highly prone to natural disasters. The outputs of this study could be used in site selection studies, designing erosion prevention systems and protecting existing human-made structures.

Keywords: Koyulhisar; Debris flow; Flow path assessment; Heuristic method; Landslide susceptibility mapping; Geographical Information System (GIS)

Introduction

Natural hazards cause much loss of life and property in the world. Studies about weather forecasting systems, early warning systems for tsunami and earthquake prediction are proceeding. Determination of source areas of avalanches, landslides and similar natural disasters is essential for risk assessment studies. The landslide is the most common type of natural disaster after the earthquakes in Turkey. Disaster risk is high in flow-type landslides, which is one of the landslide types of generally and widely accepted landslides classification of Varnes (1978). Debris flow and debris avalanche, which are flow types of a mass movement, cause significant loss of life and property due to the occurrence rates. Debris flow is a fast-moving type of flow that contains water and debris-like material (Guo and Wu 2015). Especially slope and water content are the most critical factors controlling movements of flow (Takahashi 2007; Ulusay 2007).

Turkey, which is located in a tectonically active region, has been significantly affected by earthquakes and mass movements. The North Anatolian Fault (NAF), which is the most seismically active fault of Turkey, passes through the study area. Landslide events are frequently observed due to this location. Flow type landslide is

Received: 08-Feb-2019

Revised: 13-Jul-2020

Accepted: 14-Sep-2020

one of them.

Generally, landslide damages can be decreased by predicting future landslide locations (Pradhan 2010). One of the methods of reducing landslide damages is to limit the development of settlements in landslide susceptible areas by using landslide susceptibility maps (LSM). Landslide susceptibility mapping is crucial in this sense. Many methods are used to assess the susceptibility of landslides. These methods can be classified as a heuristic, statistical, and deterministic. In this study, the heuristic method was used. This method is based on expert opinion. Experts use their knowledge to determine the weighting value of conditioning factors (Francipane et al. 2014; Leoni et al. 2015; Blais-Stevens and Behnia 2016; Abuzied et al. 2016; Bee et. al 2019; Abuzied and Alrefae 2019; Abuzied and Pradhan 2020).

On 15 March 2005, a landslide occurred in the study area, resulting in the death of 15 people. Investigations carried out in this context has increased after this landslide in the study area and its vicinity (Erik and Yilmaz 2005; Gürsoy et al. 2005; Ulusay et al. 2007; Polat and Gürsoy 2014; Polat and Tatar 2017).

Landslides susceptibility studies were carried

out in the study area and its vicinity by various authors. In Gökçeoğlu et al. (2005), a landslide inventory map was produced. LSM was constructed by the conditional probability approach. In Yilmaz (2009), an artificial neural network (ANN) model was used to produce LSM for Koyulhisar (Sivas-Turkey) region. In another study conducted by Yilmaz (2010), different methods such as conditional probability (CP), logistic regression (LR), ANN and support vector machine (SVM) were compared. In Demir (2016), Frequency Ratio (FR) and Index of Entropy methods were used for creating LSM between the southeast Reşadiye to Koyulhisar, Sivas province.

The purpose of this work is the construction of Geographical Information System (GIS)-based debris flow susceptibility map, calculating propagation and runout the distance of debris flows in the study area. Flow-R (Horton et al. 2013) software was used for calculating propagation and runout distance of debris flow.

1 Materials and Methods

This study consists of two parts. In the first

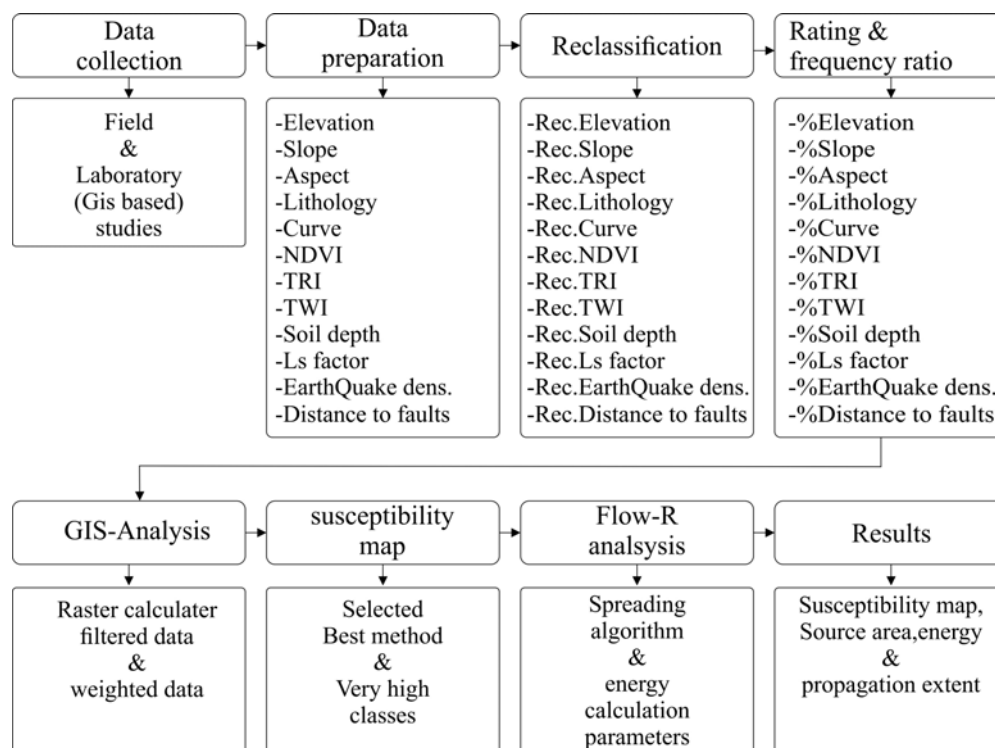


Figure 1 Workflow diagram of assessment of debris flow susceptibility and propagation.

part a susceptibility map is created, and in the second part the propagation areas of debris flow are determined. The heuristics method was used to create LSM. The propagation and runout distance of debris flows were calculated by Flow-R software. This study consists of eight main steps. These steps are described in detail at flow chart shown in Figure 1.

1.1 Study area

The study area is located to 165 km northeast of Sivas city. This area lies between 40°24'51.44" and 40°13'16.39" latitudes; and 37°28'2.8" and

37°52'25" longitudes covering an area about of 370.649 km² (Figure 2). Koyulhisar town is in the eastern part of the study area. North Anatolian Fault Zone (NAFZ), which is the major tectonic feature of Turkey, passes through the study area.

NAF is one of the most well-known strike-slip faults in the world due to its seismic activity. NAF is not a single fault plane. It is a zone formed as many right-lateral strike-slip planes and parts (Ketin 1969). This fault zone between Niksar and Koyulhisar region is called the Kelkit segment. Typical active fault morphology is observed in the study area. Kelkit valley, which extends along the fault line, was formed by the NAFZ. There are

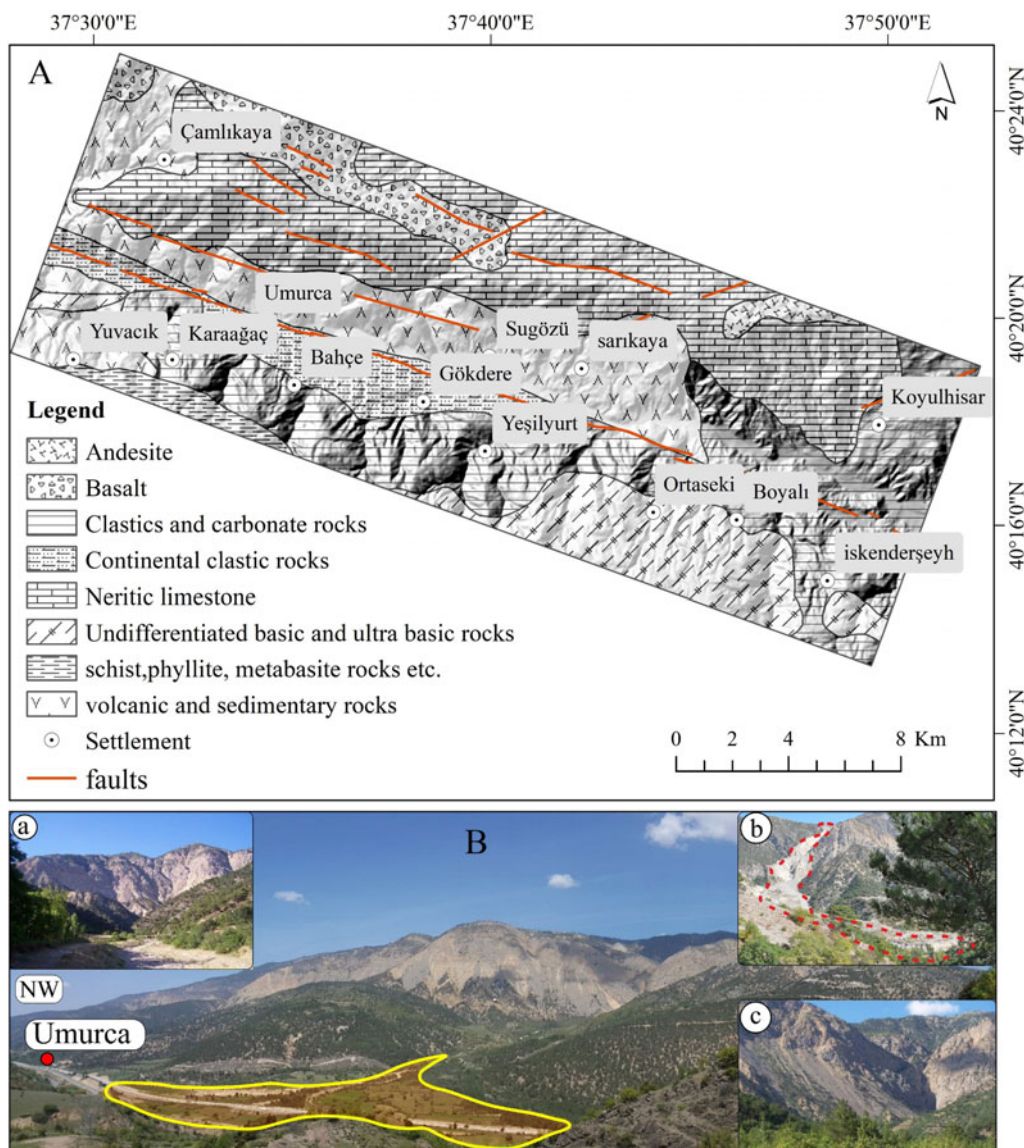


Figure 2 A) Geological map of study area, B) Paleo-flows and alluvial fan (40°19'40.10" N, 37°35'41.96" E) a: North of the Umurca village (40°20'39.36" N, 37°34'20.46" E) b: Sugözü landslide (40°20'07.28" N, 37°38'13.36" E) c: North of the alluvial fan (40°20'30.84" N, 37°36'1.97" E).

younger valleys that extend vertically to the north and south of the Kelkit valley. The lowest elevation is 537 m and the highest is 2182 m in the region. Plateau plains are observed higher than 1700 m elevation in the north.

Geological Map of General Directorate of Mineral Research and Exploration (Akbaş et al. 1991) was used to identify geological units. The Upper Paleozoic-Trias aged rocks such as schist, phyllite and metabasite are found at the base. Mesozoic aged undifferentiated basic and ultrabasic rocks are observed over these units. Upper Cretaceous aged volcanic and sedimentary rocks are located on this unit. Most of the northern part of the study area consists of Upper Cretaceous Eocene neritic limestones. The vast majority of the southern part is composed of Eocene aged clastic and carbonate rocks. Pliocene aged andesite, basalt, and continental clastic rocks cover the other older units (Figure 2A).

Paleo-flows are observed mainly in the north of the study area (Figure 2B). These flows are composed of limestone derived materials. The limestones affected by the NAFZ have fragmented-fractured structures due to shear stresses resulted from faulting. Versatile-random joint fracture systems have developed and layered structures preserved in this unit. According to Erik and Mutlutürk (2008), old mass movements observed in the study area are generally defined as debris flow based on the material type and landslide geometry.

Talus and fault terrace sediments, especially in the Plio-Quaternary Koyulhisar Formation, become active due to faults and generate landslides by moving on the water saturated ground (Tatar et al. 2000). Mass movement is observed as debris flow (Cruden and Varnes 1996), mostly in northern Koyulhisar, commonly after an intense winter (Hastaoğlu et al. 2018). The recent landslide occurred north of the Sugözü village on 17.05.2005 in the region (Figure 2B-b). This landslide caused 15 people to die, and about 30 houses destroyed.

1.2 Data preparation

Elevation, slope, aspect, curve, Normalized Difference Vegetation Index (NDVI), lithology, Topographic Roughness Index (TRI), Topographic Wetness Index (TWI), Slope Length and Steepness factor (LS-factor), soil depth, earthquake density

and distance to faults were used as input parameters for constructing the susceptibility map. The GIS-based analysis was performed by ArcGIS 10.3.1 (ESRI 2011) software. The Shuttle Radar Topography Mission Digital Elevation Model (SRTM DEM) data with 30 m spatial resolution, was used to extract some topographic features. Slope, aspect, curve, TRI, TWI, and Ls factor data were derived from SRTM DEM. NDVI data were obtained from Landsat 8 TM image. The controlling factors used in the modeling process are shown in Figure 3. All parameters were reclassified with convenient values. These parameters are explained in detail below.

Lithology: Field observation and satellite image showed that debris flows are observed on particular geological units in the study area. So, all geological units were not used in the susceptibility analysis. These units were simplified into four groups (Table 1).

Table 1 Simplified geological units in the study area

Simplified groups	Units in geological map
Group 1	Serpentinite, schist, melange, and others
Group 2	Basalt, sandstone-mudstone-limestone
Group 3	Volcanite-sedimentary rocks
Group 4	Limestone

Elevation: Elevation value is frequently used in this type of studies. According to the field observations and satellite image analysis, lower than 700 m and higher than 1950 m elevation data were not taken into consideration. The authors have created nine classes for elevation data, as shown in Table 2.

Slope angle and aspect: The slope angle and aspect angle are powerful parameters of LSM. These parameters were scored based on the kinematic analysis results. The kinematic analysis method is used in preliminary evaluations of slope stability. The angle between the slope direction and major discontinuity set direction must be smaller than $\pm 30^\circ$ in order to create failure as toppling (Hoek and Bray 1981). However, the internal friction angle of the discontinuity is also a decisive factor on the slope angle. In this study, $\phi = 30$ was used for kinematic analyses, slope angle, and aspect (dip direction) were determined using the inversion analysis. The boundary conditions proposed by Hoek and Bray were evaluated, and the aspect and slope angles of the potential failure

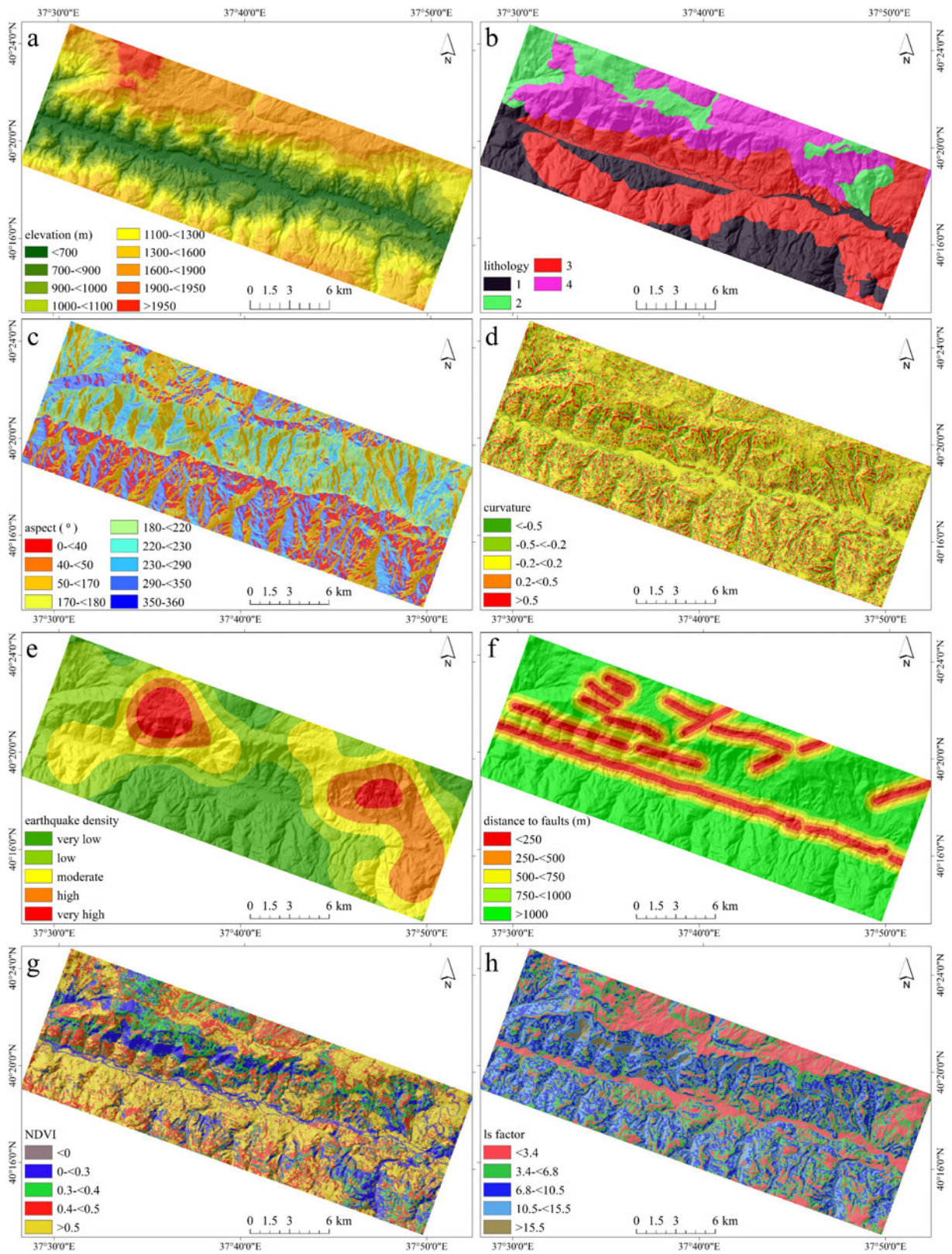


Figure 3 Debris flow controlling factors. a-elevation, b-lithology, c-aspect, d-curvature, e-earthquake density, f-distance to faults, g-Normalized Difference Vegetation Index (NDVI), h-Slope Length and Steepness factor (LS-factor). (-To be continued-)

(-Continued-)

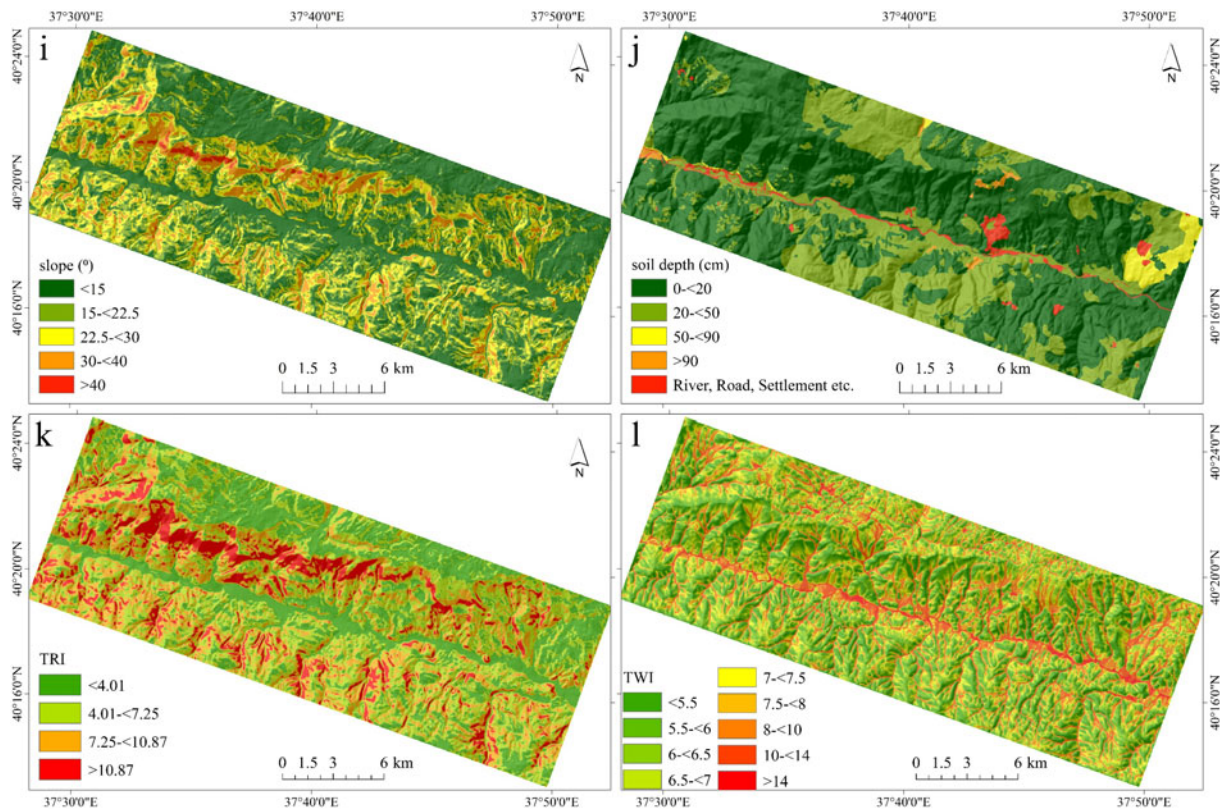


Figure 3 Debris flow controlling factors. i-slope, j-soil depth, k-Topographic Roughness Index (TRI), l-Topographic Wetness Index (TWI).

surfaces were identified.

The type of failures in the limestone is mostly observed as toppling and falling. It is concluded that these failures are discontinuity-controlled due to the effects of the NAFZ. Directions of discontinuities were measured in different locations in order to determine the probable failures in the study area. The discontinuities observed in the field are partially protected layer surfaces and random joints. It was determined that the major discontinuity systems in the measurements made from the surface of the protected layer surfaces were dip/dip direction B1: 60°/200° and B2: 50°/20° (Figure 4a, 4b, 4c).

$$NDVI = \frac{NIR-Red}{NIR+Red} \quad (1)$$

where NDVI is Normalized Difference Vegetation Index, NIR is Near Infrared Band (band 5), and Red is Red Band (band 4) of Landsat 8 image. NDVI values were reclassified for detecting the forest area between zero and 0.6. It was compared with satellite image, and best class values were determined. The authors used the curvature as a controlling factor of the susceptibility index. A

positive value indicates that the surface is convex; a negative value indicates that the surface is concave. If the value is zero, this means that the surface is linear. It was reclassified as between -0.5 and 0.5.

Topographic Roughness Index: TRI is the difference between the value of a cell and the mean of an 8-cell neighbourhood of surrounding cells. TRI formula was used given below (Riley et al. 1999);

$$TRI = \sqrt{|h_{max}^2 - h_{min}^2|} \quad (2)$$

where TRI is Terrain Ruggedness Index or Topographic Roughness Index, h_{max} is maximum topographic height, and h_{min} is minimum topographic height. The authors classified TRI values as <4.01, 4.01-7.25, 7.26-10.87, >10.87. After classification, it was observed that the TRI result is nearly compatible with the probable debris flow area shown on the field and the satellite image.

Slope length and slope angle (LS-factor): Slope length and slope angle have the most considerable influence on soil loss. The L-factor defines the impact of slope length, and the S-factor measures the effect of slope steepness. The LS-factor

Table 2 Weights of parameters and sub-parameters used to construct landslide susceptibility maps (LSM)

Parameter	Class	Rate	% Weight	Total Weight	Parameter	Class	Rate	% Weight	Total Weight
Elevation (E, m)				(Et)	Aspect (A, °)				(At)
< 700	1	0		0	0-40	1	5		25
700-<900	2	1		5	40-<50	2	2		10
900-<1000	3	2		10	50-<170	3	1		5
1000-<1100	4	3		15	170-<180	4	2		10
1100-<1300	5	4	5	20	180-<220	5	5	5	25
1300-<1600	6	5		25	220-<230	6	2		10
1600-<1900	7	3		15	230-<290	7	1		5
1900-<1950	8	2		10	290-<350	8	1		5
>1950	9	0		0	350-360	9	5		25
Slope (S, °)				(St)	Curve (C)				(Ct)
<15	1	0		0	<-0.5	1	0		0
15-<22.5	2	2		40	-0.5-<-0.2	2	2		2
22.5-<30	3	3	20	60	-0.2-<0.2	3	0	1	0
30-<40	4	4		80	0.2-<0.5	4	2		2
>40	5	5		100	>0.5	5	5		5
Lithology (L)				(Lt)	NDVI (N)				(Nt)
Group 1	1	1		10	<0	1	0		0
Group 2	2	2		20	0-0.3	2	5		35
Group 3	3	5	10	50	0.31-0.4	3	4	7	28
Group 4	4	1		10	0.41-0.5	4	1		7
					>0.5	5	0		0
TRI (Tr)				(Trt)	LS factor (F)				(Ft)
<4.01	1	0		0	<3.4	1	0		0
4.01-<7.25	2	1		15	3.4-6.8	2	2		14
7.25-<10.87	3	4	15	60	6.81-10.56	3	5	7	35
>10.87	4	5		75	10.57-15.57	4	4		28
					>15.57	5	0		0
TWI (Tw)				(Twt)	Soil depth (Sd, cm)				(Sdt)
<5.5	1	5		5	0-20	1	5		60
5.5-<6	2	4		4	21-50	2	2		24
6-<6.5	3	3		3	51-90	3	1	12	12
6.5-<7	4	2		2	>90	4	0		0
7-<7.5	5	1	1	1	River, road, etc.	5	0		0
7.5-<8	6	1		1					
8-<10	7	1		1					
10-<14	8	0		0					
>14	9	0		0					
Earthquake density (Ed)				(Edt)	Distance to faults (Df, m)				(Dft)
<0.06	1	1		12	<250	1	5		25
0.06-<0.18	2	2		24	250-<500	2	4		20
0.18-<0.30	3	3	12	36	500-<750	3	3	5	15
0.30-<0.46	4	4		48	750-<1000	4	2		10
>0.46	5	5		60	>1000	5	1		5

calculation was performed using the original equation proposed by [Boehner and Selige \(2006\)](#) and implemented using the System for Automated Geoscientific Analyses (SAGA) software. LS data were classified into five classes and rated as shown in [Table 2](#).

Earthquake density: This parameter is a triggering parameter of landslides. Firstly, rockfalls occur at steep slopes with the effect of earthquakes.

Then devastating debris flows could be developed due to the runoff ([Abuzied and Pradhan 2020](#)). Earthquake data from 1900 to the present have been used, and five classes were created by the equal interval method.

Distance to faults: The study area is located on NAF which is an active fault zone. This fault has a major role in shaping the region structurally. The geological units were affected by the NAF due to

shear stresses. Buffers with 250 m intervals were applied to the faults in the study area. Faults more than one km away were grouped in the same class.

Soil depth: This parameter is one of the considerable factors for assessing the stability of the soil and landslide susceptibility. Due to the increase in soil depth, the tendency of the soil to absorb moisture increases. This causes the runoff rate to decrease. Therefore, shallow soil is considered to be more unstable and prone to landslide than the deep soil (Sharma et al. 2012). Soil depth is derived from the map of major soil groups (Ministry of Agriculture and Forestry).

1.3 Heuristic method

The heuristic is a method derived from experience with similar problems, using readily accessible (Pearl 1984; Emiliano 2015). This method is based on expert opinion. Experts use their knowledge to define the weight of conditioning factors. The weighting process is extremely subjective. Conditioning factors should be determined by considering past events. Before the scoring process, a detailed field study supported by satellite images and GIS-based studies is required. After experts determine the effect of each factor on the landslides occurrence, the sub-parameters should be scored.

In this study, 12 conditioning factors were selected for constructing LSM. These factors were weighted with the help of field surveys and GIS-based studies, and inventory data were not taken into account. Scoring was made with the help of field surveys and GIS-based studies, and inventory data were not taken into account. The parameters are weighted in percentage. The effects of the parameters were ranked as low, medium, high and

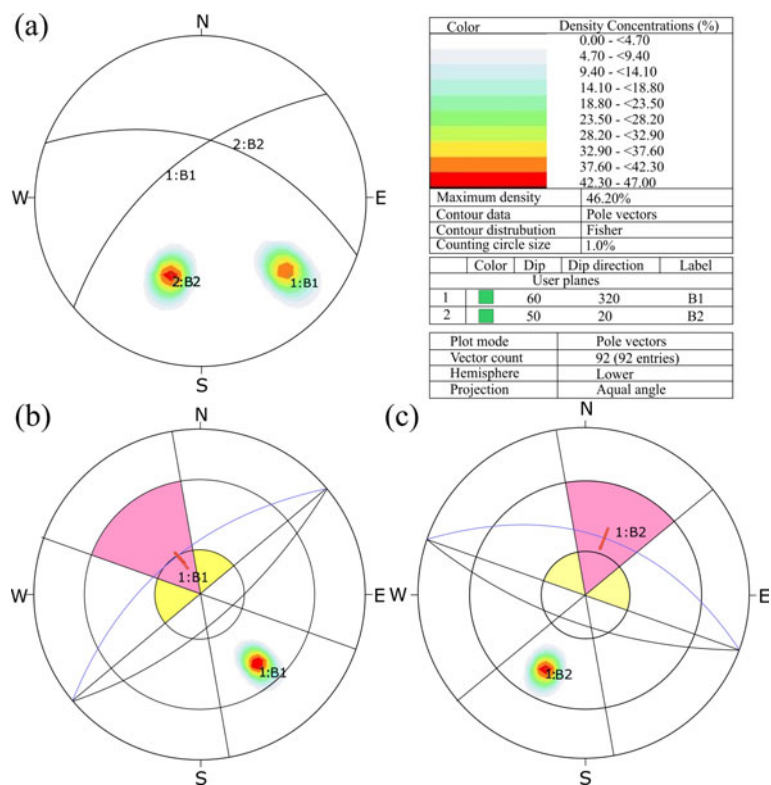


Figure 4 (a) Distribution of the major discontinuities in the study area, (b) Kinematic assessment of B1, (c) Kinematic assessment of B2

very high. Weights of percentage were assigned to parameters considering to this order. The slope parameter was weighed as 20% for this study area. This is the maximum weight.

The smallest weight value of one is assigned to the TWI and Curve parameters. The other parameters were weighted as 15, 12, 12, 10, 7, 7, 5, 5, 5 for TRI, soil depth, earthquake density, lithology, NDVI, Ls-factor, elevation, aspect, distance to faults, respectively. Sub-parameters were rated between 0 and 5 in the same way (Table 2).

1.4 Constructing susceptibility map

All weighted 12 parameters were compiled and processed on the ArcGIS platform. Total weight values were assigned to all parameters, and new raster data were created. They were integrated using;

$$SI = Et + At + St + Ct + Nt + Trt + Ft + Twt + Sdt + Edt + Dft \quad (3)$$

where SI is Susceptibility index, Et elevation data, At slope direction data, St slope angle data, Ct curvature data, Lt lithological data, Nt NDVI data,

Trt TRI data, Ft LS factor data, Twt TWI data, Sdt soil depth data, Edt earthquake density data and Dft distance to faults data.

LSM of the area was constructed by this method and reclassified as very low, low, moderate, high, and very high classes by using the equal area method. In order to calculate the propagation areas, the initiation areas should be determined. For this purpose, very high-class areas of the LSM were selected as initiation (source) area of debris flow. To create a more accurate source area data, filter rasters have been created for some parameters including zero value in total weight values such as elevation, slope, soil depth, Ls-factor, NDVI, CRV, TRI, and TWI. A binary raster file is obtained by assigning one to non-zero cells. The final filtered raster file (FT) was created by multiplying the rasters with each other. Thanks to these rasters, all cells with the value of zero are ignored. Thus, the source area map has been simplified. While the source cell number before filtering was 27809, it became 13052 after filtering.

The final source area data was obtained by multiplying FT and SI data on the ArcGIS platform.

$$SA = FT \times SI_{source} \quad (4)$$

where SA is the source area of debris flow, FT is final filtered data, and SI_{source} is very high value of susceptibility index.

1.5 Calculating Propagation and runout distance of debris flows

This analysis was implemented by Flow-R software developed by Horton et al. (2013) at the University of Lausanne. Two types of algorithms are used to assess propagation (Horton et al. 2013). These are spreading algorithms and friction laws. Spreading algorithms control the path and the spreading of the debris flows. Friction laws determine the runout distance. Flow direction algorithms control the spreading. The software has several flow direction algorithms. However, not all of them are related to debris flow assessment. Flow-R software proposes Holmgren's (1994) flow direction algorithm or its modified version for debris flows. In the Holmgren algorithm, an x value is added to the multiple flow direction algorithm. This value controls divergence:

$$P_i^{fd} = \frac{(\tan\beta_i)^x}{\sum_{j=1}^8 (\tan\beta_j)^x} \forall \begin{cases} \tan\beta > 0 \\ x \in [1; +\infty[\end{cases} \quad (5)$$

where i and j are the flow directions, P^{fd} is the susceptibility proportion in direction i , $\tan\beta_i$ is the slope gradient between the central cell and the cell in direction i , and x is the variable exponent.

The exponent of the Holmgren algorithm has a substantial effect on the spreading. These exponents are commonly applied to a range of four and six. We tested the value of four and six. The outcomes were compared with mapped debris flow on the field. The exponent of six showed satisfactory results. Therefore, this value was selected as exponent of the Holmgren algorithm for our simulation.

The modified version of Holmgren's (1994) was used in this study. Horton et al. (2013) changed the height of the inner cell by a parameter dh . This parameter changes the gradient's values. Factor dh allows smoothing of DEM roughness and production of more consistent spreading, particularly in the case of high-resolution data. We used in our study 20x20 m resolution DEM data and thus dh value was used as equal to one.

The purpose of persistence function is to create a new behaviour of inertia. This function weights the flow direction using the changes in direction for the previous direction (Gamma 2000). We selected Gamma 2000 weights for the inertial algorithm.

Since no mass information, the mass of the flow is considered as a unit value. The energy required to travel to another cell must be calculated. Energy is the controlling factor for runout distance (Horton et al. 2013). It can be calculated as shown in the equation below:

$$E_{kin}^i = E_{kin}^0 + \Delta E_{pot}^i - E_f^i \quad (6)$$

where E_{kin}^i is the kinetic energy of the cell in direction i , E_{kin}^0 the kinetic energy of the central cell, ΔE_{pot}^i the change in potential energy to the cell in direction i , and E_f^i the energy lost in friction to the cell in direction i .

In this study, Perla's (1980) two-parameter friction model was used for the computing of runout distance. This formula is given below:

$$\begin{aligned} v_i &= (a_i \omega (1 - \exp b_i) + v_0^2 \exp b_i)^{\frac{1}{2}}, \\ &\text{with} \\ a_i &= g(\sin\beta_i - \mu \cos\beta_i) \\ b_i &= \frac{-2L_i}{\omega} \end{aligned} \quad (7)$$

where β_i is the slope angle of the segment, v_0 the

velocity at the beginning of the segment, L_i the length of the segment, g the acceleration due to gravity, μ the friction parameter and ω the mass-to-drag ratio.

This model was improved for avalanches but has also been used for debris flows (Zimmermann et al. 1997). Parameters ω and μ control the runout distance. We kept the other parameters fixed and we tried different ω and μ values. The results showed that the runout distance was more sensitive to the friction coefficient rather than the mass-to-drag ratio. We selected ω value as 200 and μ value as 0.02 because they provided the best fit for mapped debris flows.

2 Results and Discussion

Various methods are used in the assessment of landslide susceptibility. In this study, the GIS-based heuristic method was used to construct LSM. Elevation, slope, aspect, curve, NDVI, lithology, TRI, TWI, LSfactor, soil depth, earthquake density and distance to faults were used as parameter for analysis. These parameters were weighted based on experience. The slope angle and aspect angle were scored by values obtained using kinematic analysis. This map was classified by an equal interval method by five classes (very low, low, moderate, high, and very high) (Figure 5). The very high landslide susceptible zones cover 6% of the study area. It is mostly located along the north of the valley. This area largely consists of weathered and fractured, Upper Cretaceous-Eocene neritic limestones. 27% of the study area corresponds to high landslide susceptible zones. These zones are observed on the steep topography of the north and south slopes. The moderate, low and very low-susceptible zones occupy 27%, 31%, and 6%, respectively. The areas corresponding to high and very high zones of susceptibility map are compatible with the paleo debris flow areas defined in the field. These areas mostly correspond to the limestone units found on steep slopes. This situation shows the relationship between tectonism and lithology in the region. ROC curve was used to assess the performance of LSM. 34 paleo debris flows are mapped in the study area. 30 percent of data (10) were randomly selected as test data and the others (24) were selected as training data. The

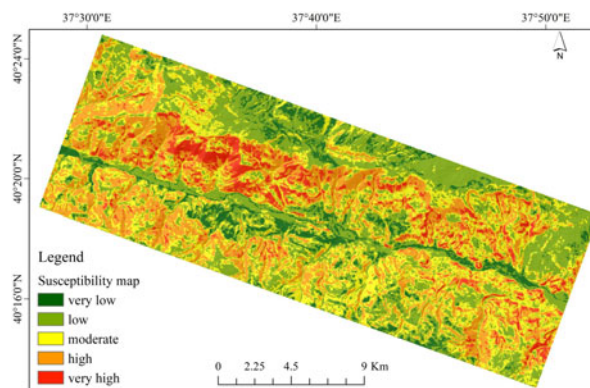


Figure 5 Debris flow susceptibility map of the study area.

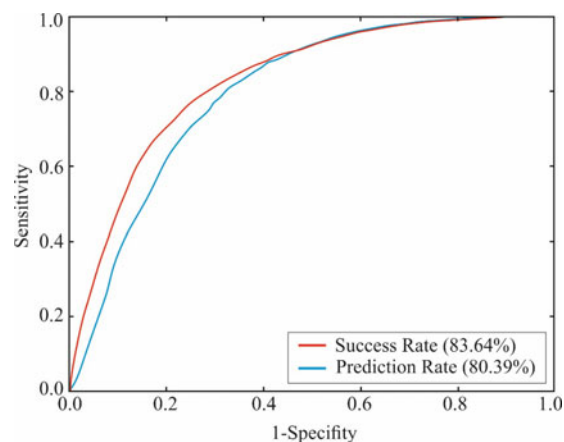


Figure 6 The area under curve values of landslide susceptibility map.

area under curve AUC value was calculated as 83.64% and 80.39% for the success rate and prediction rate, respectively (Figure 6). Overall, the AUC value varies from 0.5 to 1. As the AUC value equals to 1, the performance of landslide models is perfect. Contrarily, if the AUC value equals to 0.5, the performance of landslide models is inaccurate. The AUC value of 0.80 for the prediction rate indicates a reasonable value. Flow-R software was used for the assessment of the probability of propagation extent, and runout distance of debris flows. This software also can detect source areas using a variety of parameters. In this study values corresponding to very high areas of LSM were selected as the source area. As a result, the propagation (Figure 7a) and runout distances (Figure 7b) of the debris flow in the region have been calculated. Propagation map was categorized into five classes: very low, low, moderate, high, and very high probability zones. 5% of the source area corresponds to the very high probability class and

located in the streams. The high and moderate probability classes match 13%, 16% of the source area, respectively. These zones are mostly observed slopes of the valleys. The low and very low probability classes commonly are located in lower elevation. 19% of the source area has low probability propagation extend. The very low zones correspond 44% of the source area. They mostly cover the paleo debris flow fans. Propagation of flows may not precisely compatible with paleo debris flows. This is expected, because debris flow events may have occurred many times and exposed to different geographical, geological, and climatic conditions in the past years. Flow-R method reflects present-day conditions. Sugözü landslide occurred on 17.03.2005, is almost compatible with the Flow-R result. Runout distance is based on kinetic energy calculation. This data fits with the debris flow inventory data. The regions having high energy are compatible with the paleo landslide occurrences. Paleo debris flows are observed mostly in the north of the study area. 34 paleo flows were mapped in the region, and 28 of them are located in north section of the valley (Figure 7b).

Debris flow is a fast-moving type of landslides. Therefore, it causes a significant loss of life and property. Especially man-made structures located on the flow route are in danger. A village was completely destroyed in the Kuzulu landslide (March 2005) that occurred in the study area. Many of the debris flow have a long travel distance. This feature increases the hazard rates of flows in the region.

3 Conclusions

The study area, located on an active fault zone NAFZ, is highly prone to natural disasters. Landslide is the second common disaster after the earthquake in the region. Debris flow, one of the

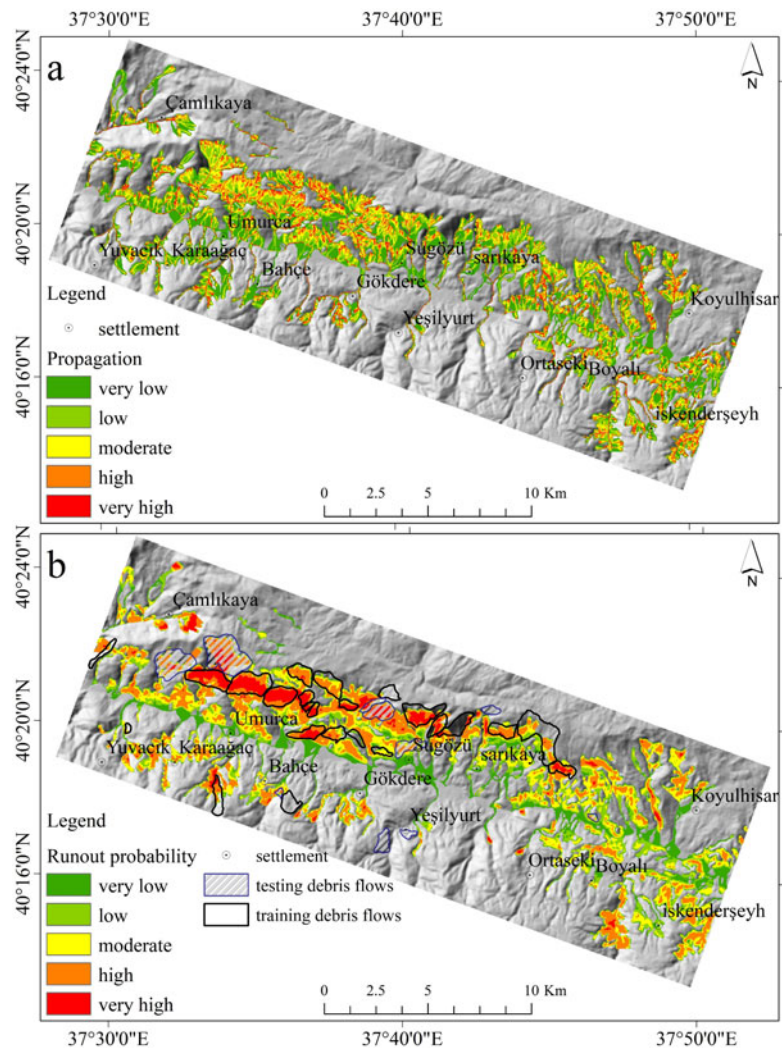


Figure 7 a-Propagation of debris flows, b-runout distance (Probability) of debris flows and testing - training debris flows.

types of the landslide, was mostly observed in the north of the study area. The purpose of this study is to determine the source area, propagation, and runout distance of debris flows.

In this study, only the heuristic method was used to construct the LSM. The source areas of debris flows were derived from this map. Therefore, it is important to create a high accuracy LSM. The AUC value was calculated as 0.80 for the prediction rate and this indicates a reasonable value. Since the heuristic method is completely subjective, the results may vary according to the users. In future studies, a detailed debris flow inventory map can be prepared and using statistical or machine learning methods can be compared with this method.

There are many human-made structures, such

as settlements, roads, and water channels in the study area. The outcomes of this study (susceptibility map, propagation, and runout distance of debris flows) are significant for decision makers at the region located on an active fault zone (NAFZ). It is also crucial for the in terms of erosion prevention studies because debris flow causes erosion, and the carried material fills the Kelkit valley located in the region.

References

- Abuzied S, Ibrahim S, Kaiser M, Saleem T (2016) Geospatial susceptibility mapping of earthquake-induced landslides in Nuweiba area, Gulf of Aqaba, Egypt. *Journal of Mountain Science* 13: 1286-303.
<https://doi.org/10.1007/s11629-015-3441-x>
- Abuzied SM, Alrefae HA (2019) Spatial prediction of landslide-susceptible zones in El-Qaá area, Egypt, using an integrated approach based on GIS statistical analysis. *Bulletin of Engineering Geology and the Environment* 78: 2169-2195.
<https://doi.org/10.1007/s10064-018-1302-x>
- Abuzied SM, Pradhan B (2020) Hydro-geomorphic assessment of erosion intensity and sediment yield initiated debris-flow hazards at Wadi Dahab Watershed, Egypt. *Georisk: Assessment and Management of Risk for Engineered Systems and Geohazards* 1-26.
<https://doi.org/10.1080/17499518.2020.1753781>
- Akbaş B, Akdeniz N, Aksay A, et al. (1991) Turkey geology map. General Directorate of Mineral Research and Exploration Publications. Ankara Turkey. (In Turkish)
- Bee EJ, Dashwood C, Pennington C, et al. (2019) Creating a national scale debris flow susceptibility model for Great Britain: a GIS based heuristic approach 2. *Natural Hazards and Earth System Sciences*. Discuss.
<https://doi.org/10.5194/nhess-2019-54>
- Blais-Stevens A, Behnia P (2016) Debris flow susceptibility mapping using a qualitative heuristic method and Flow-R along the Yukon Alaska Highway Corridor, Canada. *Natural Hazards and Earth System Sciences* 16(2): 449-462.
<https://doi.org/10.5194/nhess-16-449-2016>
- Boehner J, Selige T (2006) Spatial prediction of soil attributes using terrain analysis and climate regionalisation. In: Boehner, J., McCloy, K.R., Strobl, J.: 'SAGA - Analysis and Modelling Applications', Goettinger Geographische Abhandlungen 115: 13-27
- Cruden DM, Varnes DJ (1996) Landslide types and processes. In: Turner AK, Schuster RL (eds) *Landslides investigation and mitigation*. Transportation research board, US National Research Council. Special Report 247, Washington, DC, Chapter 3, pp. 36-75
- Demir G (2016) Landslide susceptibility assessment of the part of the North Anatolian Fault Zone (Turkey) by GIS-based frequency ratio and index of entropy models. *Natural Hazards and Earth System Sciences*.
<https://doi.org/10.5194/nhess-2016-327>
- Emiliano I (2015) *Heuristic Reasoning: Studies in Applied Philosophy, Epistemology and Rational Ethics*. Switzerland: Springer International Publishing. pp 1-2.
<https://doi.org/10.1007/978-3-319-09159-4>
- Erik D, Mutlutürk M (2008) Yukarı Kelkit vadisi Koyulhisar-Reşadiye arasındaki paleo moloz akmaları. IX. Bölgesel Kaya Mekaniği Sempozyumu, Dokuz Eylül Üniversitesi, İzmir. (In Turkish)
- Erik D, Yılmaz H (2005) 17.03.2005 Kuzulu (Sugözü-Koyulhisar-Sivas) moloz çığı. 58. Türkiye Jeoloji Kurultayı, 11-17 Nisan 2005 Bildiri Özleri kitabı, 179-180, Ankara. (In Turkish)
- ESRI (2011) *ArcGIS Desktop: Release 10*. Redlands, CA: Environmental Systems Research Institute
- Francipane A, Arnone E, Lo Conti F, et al. (2014) A comparison between heuristic, statistical, and data-driven methods In landslide susceptibility assessment: An application to the Briga and Giampilieri catchments. CUNY Academic Works.
https://academicworks.cuny.edu/cc_conf_hic/150
- Gamma P (2000) DF-Walk: Ein murgang-simulationsprogramm zur gefahrenzonierung (Geographica Bernensia, G66). University of Bern. (In German)
- Gokceoglu C, Sönmez H, Nefeslioglu HA, et al. (2005) The March 17, 2005 Kuzulu landslide (Sivas, Turkey) and landslide susceptibility map of its near vicinity. *Engineering Geology* 81: 65-83.
<https://doi.org/10.1016/j.enggeo.2005.07.011>
- Guo X, Wu W (2015) Some ideas on constitutive modeling of debris materials in: Wu, W (Ed.), *Recent Advances in Modeling Landslides and Debris Flows*. Springer International Publishing, Switzerland pp 1-9.
<https://doi.org/10.1007/978-3-319-11053-0>
- Gürsoy H, Tatar O, Mesci L, Koçbulut F (2005) KAFZ üzerinde gelişen 17 Mart 2005 Kuzulu mahallesi Heyelanının (Sugözü Köyü - Koyulhisar, Sivas) jeolojik, jeomorfolojik özellikleri ve mevcut risk durumu. ATAG-9 Toplantısı, Bildiri özleri Kitabı, Sivas. pp 44-45. (In Turkish)
- Hastaoğlu KÖ, Poyraz F, Türk T, et al. (2018) Investigation of the success of monitoring slow motion landslides using Persistent Scatterer Interferometry and GNSS methods. *Survey Review* 50(63):475-486.
<https://doi.org/10.1080/00396265.2017.1295631>
- Hoek E, Bray JW (1981) *Rock Slope Engineering*. Revised 3rd edition. The Institution of Mining and Metallurgy, London. pp 341 - 351
- Holmgren P (1994) Multiple flow direction algorithms for runoff modeling in grid based elevation models: An empirical evaluation. *Hydrological Processes*, 8(4): 327-334.
<https://doi.org/10.1002/hyp.3360080405>
- Horton P, Jaboyedoff M, Rudaz B, Zimmermann M (2013) Flow- R, a model for susceptibility mapping of debris flows and other gravitational hazards at a regional scale. *Natural Hazards and Earth System Sciences* 13: 869-885.
<https://doi.org/10.5194/nhess-13-869>
- Ketin İ (1969) Kuzey Anadolu Fayı hakkında. *Maden Tetkik ve Arama Dergisi*. 72:1-27. (In Turkish)
- Leoni G, Campolo D, Falconi L, et al. (2015) Heuristic method for landslide susceptibility assessment in the Messina municipality. In *Engineering Geology for Society and Territory - Volume 2: Landslide Processes* Springer International Publishing 2:501-504.
https://doi.org/10.1007/978-3-319-09057-3_82
- Pearl J (1984) *Heuristics: Intelligent search strategies for computer problem solving*. New York, Addison-Wesley. p 382.

- Perla R, Cheng TT, McClung DM (1980) A two-parameter model of snow-avalanche motion. *Journal of Glaciology* 26: 197-207. <https://doi.org/10.3189/S002214300001073X>
- Polat A, Gürsoy H (2014) Sayısal Yükselti Modeli (SYM) verileri yardımıyla 17 Mart 2005 Kuzulu (Koyulhisar, Sivas) heyelanının hacim hesabı. ATAG 18. Muğla, Sıtkı Koçman Üniversitesi. (In Turkish)
- Polat A, Tatar O (2017) 2D simulation of probable debris flow in Koyulhisar, Turkey. *International Symposium on Gis Applications in Geography and Geosciences*. Çanakkale, Turkey.
- Pradhan B (2010) Landslide susceptibility mapping of a catchment area using frequency ratio, fuzzy logic and multivariate logistic regression approaches. *Journal of the Indian Society of Remote Sensing* 38: 301-320. <https://doi.org/10.1007/s12524-010-0020-z>
- Riley SJ, DeGloria SD, Elliot R (1999) A terrain ruggedness index that quantifies topographic heterogeneity. *Intermountain Journal of Sciences* 5: 23-27.
- Sharma LP, Patel N, Debnath P, Ghose MK (2012) Assessing landslide vulnerability from soil characteristics—a GIS-based analysis. *Arabian Journal of Geosciences* 5: 789-796. <https://doi.org/10.1007/s12517-010-0272-5>
- Takahashi T (2007) Debris flow: Mechanics, prediction and countermeasures. Taylor & Francis. p 448.
- Tatar O, Aykanat D, Kocbulut F, et al. (2000) Landslide investigation and assessment report of Koyulhisar town centre and district police chief building. Faculty of Engineering, Cumhuriyet University, Sivas, Turkey (In Turkish)
- Ulusay R, Aydan Ö, Kılıç R (2007) Geotechnical assessment of the 2005 Kuzulu landslide (Turkey). *Engineering Geology* 89:112-128. <https://doi.org/10.1016/j.enggeo.2006.09.020>
- Ulusay R (2007) Heyelanlar ve mühendislik şevlerindeki duraysızlıklar: Türleri, etkileri ve zararların azaltılması. Sel-Heyelan-Çığ Sempozyumu, Samsun, Bildiriler Kitabı. pp 158-160. (In Turkish)
- Varnes DJ (1978) Slope movement types and processes, in Schuster RL, and Krizek RJ, eds., *Landslides: Analysis and control*, National Research Council, Washington, D.C., Transportation Research Board, National Academy Press, Special Report 176: 11-33.
- Yılmaz I (2009) A case study from Koyulhisar (Sivas-Turkey) for landslide susceptibility mapping by artificial neural networks. *Bulletin of Engineering Geology and the Environment* 68:297-306. <https://doi.org/10.1007/s10064-009-0185-2>
- Yılmaz I (2010) Comparison of landslide susceptibility mapping methodologies for Koyulhisar, Turkey: conditional probability, logistic regression, artificial neural networks, and support vector machine. *Environmental Earth Sciences* 61(4): 821-836. <https://doi.org/10.1007/s12665-009-0394-9>
- Zimmermann M, Mani P, Gamma P, et al. (1997) Murgangefahr und Klimaänderung - ein GIS-basierter Ansatz. NFP31 Schlussbericht. Vdf Verlag, Zürich. P. 162. (In German)